ENVIRONMENTAL BIOTECHNOLOGY

Simultaneous nutrients and carbon removal during pretreated swine slurry degradation in a tubular biofilm photobioreactor

Ignacio de Godos · Cristina González · Eloy Becares · Pedro A. García-Encina · Raúl Muñoz

Abstract The biodegradation potential of an innovative enclosed tubular biofilm photobioreactor inoculated with a *Chlorella sorokiniana* strain and an acclimated activated sludge consortium was evaluated under continuous illumination and increasing pretreated (centrifuged) swine slurry loading rates. This photobioreactor configuration provided simultaneous and efficient carbon, nitrogen, and phosphorous treatment in a single-stage process at sustained nitrogen and phosphorous removals efficiencies ranging from 94% to 100% and 70–90%, respectively. Maximum total organic carbon (TOC), NH_4^+, and PO_4^{3-} removal rates of 80 ± 5 g C m_r^{-3} day^{-1}, 89 ± 5 g N m_r^{-3} day^{-1}, and 13 ± 3 g P m_r^{-3} day^{-1}, respectively, were recorded at the highest swine slurry loadings (TOC of $1,247\pm62$ mg L^{-1}, N–NH_4^+ of 656 ± 37 mg L^{-1}, P–PO_4^{3+} of 117 ± 19 mg L^{-1}, and 7 days of hydraulic retention time). The unusual substrates diffusional pathways established within the phototrophic biofilm (photosynthetic O_2 and TOC/NH_4^+ diffusing from opposite sides of the biofilm) allowed both the occurrence of a simultaneous denitrification/nitrification process at the highest swine slurry loading rate and the protection of microalgae from any potential inhibitory effect mediated by the combination of high pH and high NH_3 concentrations.

C. González · P. A. García-Encina · R. Muñoz (✉)
Department of Chemical Engineering and Environmental Technology, University of Valladolid,
Paseo del Prado de la Magdalena s/n,
47011 Valladolid, Spain
e-mail: mutora@iq.uva.es

I. de Godos · E. Becares
Department of Biodiversity and Environmental Management,
University of León,
Campus Vegazana,
24071 León, Spain

In addition, this biofilm-based photobioreactor supported efficient biomass retention (>92% of the biomass generated during the pretreated swine slurry biodegradation).

Keywords Biofilm · *Chlorella sorokiniana* · Microalgae · Nutrients removal · Photosynthetic oxygenation · Swine slurry · Tubular photobioreactor

Introduction

Microalgae-based processes constitute a less energy intensive and more environmentally friendly alternative to conventional treatment methods (activated sludge or anaerobic systems) due to its free O_2 production and its potential for nutrients recovery (Evans et al. 1986; Wilkie et al. 2002; Tchobanoglous et al. 2003; Muñoz and Guieysse 2006). In photosynthetically oxygenated processes, microalgae supplies the O_2 required by bacteria to oxidize both organic matter and NH_4^+, while bacterial respiration provides the CO_2 needed for microalgal photosynthesis. This solar-powered symbiosis constitutes thus a cost-free oxygenation mode (Oswald 1988; Travieso et al. 2006). The nitrogen and phosphorus present in the wastewater is also effectively removed via assimilation into algal–bacterial biomass or via pH-enhanced NH_4^+ stripping and PO_4^{3-} precipitation (Nurdogan and Oswald 1995; McGriff and McKinney 1972). The CO_2 released during organic matter oxidation is assimilated into algal biomass, which helps mitigating any greenhouse effects associated to wastewater treatment (Oswald 1988). In addition, the potential valorisation of the residual algal–bacterial biomass as fertilizer, as source for CH_4 production or as supplement in animal alimentation can offset a significant fraction of process operational costs (Barlow et al. 1975).

Despite the above-mentioned advantages, microalgal-based systems still suffer from serious operational limitations derived from a poor microalgae settling (Muñoz 2005) and a potential NH_3-mediated microalgae inhibition (Gonzalez et al. 2008a). Phototrophic biofilms represent thus an innovative approach to microalgal-based treatment systems as they can allow the simultaneous production of a biomass free effluent (due to the good settling characteristics of the algal–bacterial flocs detached from the biofilm) and microalgae protection from pollutant toxicity as a result of the diffusional gradients originated within the flocs (Hoffman 1998; Nicolella et al. 2000; Wolf et al. 2007). Microalgae immobilization into carrageenan, chitosan, or alginate has been so far the only immobilization technique assessed, despite that the high structural weakness and cost of these biopolymers limits their large-scale application (Hoffman 1998). Consequently, new methods for biomass immobilization are required to support photosynthetically oxygenated processes.

This study evaluated the removal of carbon, NH_4^+, and PO_4^{3-} from pretreated piggery wastewater in an enclosed biofilm tubular photobioreactor configuration based on the natural ability of the symbiotic community to attach to photobioreactor's walls. The microalgae *Chlorella sorokiniana* and a bacterial community from a swine manure degrading activated sludge were used as model algal–bacterial consortium. *C. sorokiniana* represents one of the worst-case scenarios to enhance biomass sedimentation due to its poor settling characteristics, despite that recent studies have shown that $CaCl_2$ addition can increase the coflocculation of *C. sorokiniana* and its associated symbiotic bacteria (Imase et al. 2008). This work constitutes the natural extension of the research previously published by Gonzalez et al. (2008b), being the influence of wastewater load the key parameter evaluated. Only the soluble fraction of swine manure was herein considered in order to evaluate the real potential for organic carbon, nitrogen, and inorganic carbon assimilation (not feasible in the previous study due to the impossibility of selectively separate non-biodegraded particulate organic matter and the generated algal–bacterial biomass in the effluent).

Materials and methods

Microorganisms and culture conditions

The microalgae *C. sorokiniana 211/8k* was obtained from the culture collection of algae and protozoa of the SAMS Research Services (Argyl, Scotland) and cultivated according to Muñoz et al. (2005). The mixed bacterial culture was obtained from the secondary settler of a bench-scale swine slurry degrading activated sludge process operated with both nitrification and denitrification stages (DN configura-

tion). Prior to inoculation, both cultures were centrifuged at 6,000 rpm and resuspended in tap water.

Swine manure pretreatment and characterization

Raw swine slurry was obtained from the main collector of a swine manure treatment plant in Hornillos de Eresma (GRUPO GUASCOR, Valladolid, Spain) and stored at 4 °C. Prior to experimentation, swine slurry was centrifuged for 20 min at 6,000 rpm and 4 °C. Therefore, only the soluble fraction of carbon, nitrogen, and phosphorus was considered in the present study. Two batches of swine slurry obtained at different periods from January to April (namely batch A and B) with similar carbon, nitrogen, and phosphorous concentrations but different soluble organic carbon biodegradabilities were used to carry out the experiments described below.

Centrifuged swine slurry (CSS) biodegradability was evaluated in glass bottles of 1,250 mL (22×10.5 cm height $\times$ base diameter) filled with 100 mL of undiluted CSS and inoculated with 2 mL of acclimated activated sludge. The bottles were then closed with butyl septa, sealed with plastic caps, and incubated for 20 days at 30 °C under magnetic agitation (300 rpm). Liquid samples of 1 mL were periodically withdrawn in order to monitor the dissolved total organic carbon (TOC) concentration. Tests were carried out in duplicate for each swine slurry batch employed. Flask headspace was periodically renewed for 5 min during each sampling in order to avoid O_2 limiting conditions during CSS degradation.

Photobioreactor

The photobioreactor herein used consisted of a 14-m PVC transparent tube (25 mm ID) with a total liquid volume of 7.5 L arranged horizontally in a spiral way and illuminated at 10,000 lux using 8–40 W fluorescents lamps (Osram L, Germany) placed above the experimental set-up (Fig. 1). A 0.5-L closed storage tank (10 mm ID) was used to allow culture recirculation and effluent withdrawal. The system was operated as a complete-mixed reactor by recirculating the culture broth at 0.4 L min^{-1} (0.14 m s^{-1}) with a peristaltic pump (Watson-Marlow Bredel Pumps, Model MG06171, England) in order to avoid any potential NH_3-mediated inhibitory effect (recirculation/feed ratio$\approx$480). The photobioreactor was initially filled with tap water and inoculated with *C. sorokiniana* at 87 mg L^{-1} and acclimated activated sludge at 87 mg volatile suspended solids (VSS) L^{-1}. Biomass sedimentation was carried out in a 0.75-L settler located at the photobioreactor outlet (Fig. 1).

In a first series of experiments, the photobioreactor was operated for 3 months under continuous illumination and continuous feeding regime at 7 days of hydraulic retention
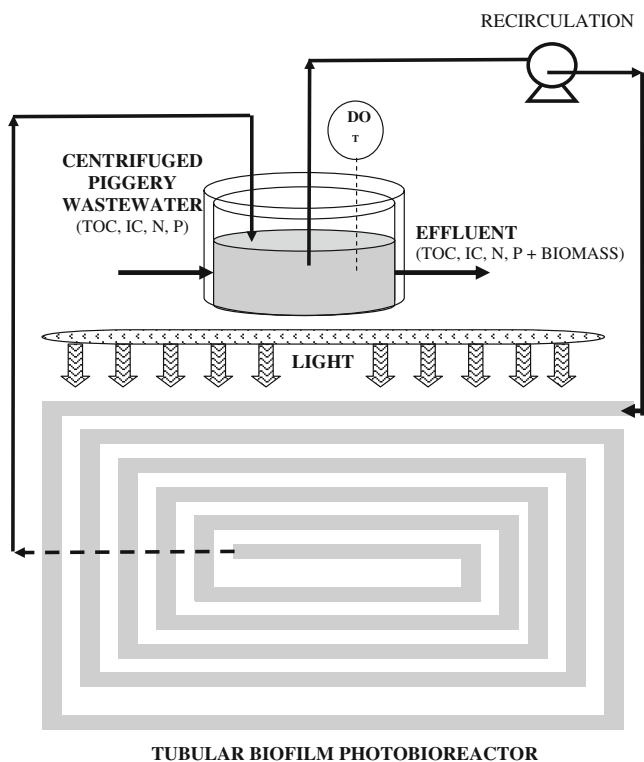
Fig. 1 Schematic diagram of the photobioreactor set-up

time (HRT) at increasing CSS loading rates (eight, four, and two times diluted and undiluted CSS, corresponding to periods I, II, III, and IV, respectively). Each loading rate was maintained for a period of 21 days. Two different batches of swine slurry were employed in this first series: batch A for periods I, II, and III and batch B for period IV. CSS dilution in periods I, II, and III was carried out using tap water, and the resulting feed was maintained at 4 °C throughout the entire experimentation in order to avoid bacterial contamination. Liquid samples of process influent (100 mL) and effluent (200 mL taken at the top of the settler) were withdrawn twice a week in order to monitor dissolved TOC, dissolved inorganic carbon (IC), NO_3^-, NO_2^-, NH_4^+, and PO_4^{3-}, and algal–bacterial biomass in the effluent was characterized as absorbance at 550 nm (OD_{550}) and VSS, effluent total suspended solids (TSS), and pH. Dissolved oxygen (DO) and temperature were monitored in situ. In addition, a 100-mL sample was taken from the bottom of the settler to estimate biomass sedimentation (VSS). Photobioreactors's effluent was also periodically monitored by microscopy to tentatively characterize the predominant microalgal species.

Analytical procedures

TOC and IC concentration was determined using a Shimadzu TOC-5050A analyzer (Japan). Liquid samples

were centrifuged at 6,000 rpm for 20 min prior to analysis. $N–NH_4^+$ concentration was determined using an ammonia Electrode, Orion 900/200 (Thermo Electron Corporation, Beverly, USA). NO_3^- and NO_2^- were analyzed via HPLC-IC (Hewlett Packard 5890 Series II) according to Standard Methods (Eaton et al. 2005). OD_{550}, used as indicator of microbial growth, was determined using a HITACHI U200 UV/visible spectrophotometer (Hitachi, Tokyo, Japan). A CRISON micropH 2002 (Crison Instruments, Barcelona, Spain) was used for pH determination. Soluble phosphorus (as orthophosphate), TSS, and VSS concentrations were determined according to Standard Methods (Eaton et al. 2005). DO and temperature in the bioreactor were determined in situ using a Multiline P4 Oxical-SL Universal Meter with an accuracy of ±0.04 mg O_2 L^{-1} (WTW, Germany). An optical microscope (Leica instruments, USA) was used for morphological microalgae characterization. The composition of gas compartment formed within the biofilm was determined via GC-TCD analysis according to Muñoz et al. (2007)

Results

The average composition of the pretreated swine slurry (CSS) was as follows (milligrams per liter): TOC 1,247± 62, IC 1,290±51, $N–NH_4^+$ 656±37, and PO_4^{3+} 117±19. CSS biodegradabilities of 54±1 and 39±2 were recorded for swine manure batch A and B, respectively. At this point, it must be stressed that differences in farm swine manure management practices and pig nutrition are often responsible of the different TOC biodegradabilities observed. In this context, biodegradable soluble organic fractions ranging from 40% to 86% have been described elsewhere in literature (Boursier et al. 2005; Gonzalez et al. 2008a; Baumgarten et al. 1999).

Despite process start-up (period I) resulted in fluctuating TOC-REs ranging from 9% to 48%, process performance achieved stable TOC removals of 61±3% and 60±6% during period II (four times diluted CSS) and III (two times diluted CSS), respectively, followed by a decrease to 44± 5% when the photobioreactor was operated with undiluted CSS (period IV; Fig. 2a). In this context, TOC elimination capacities (ECs) increased with increasing loading rates from 10±7 g TOC m_r^{-3} day^{-1} using eight times diluted CSS to 80±5 g TOC m_r^{-3} day^{-1} when fed with undiluted CSS (inlet TOC concentrations of approx. 1,200 mg C L^{-1}). Irregular IC-REs ranging from 40% to 80% were recorded during periods I and II (Fig. 2b). Further increases in CSS loading resulted in lower IC-RE (54±3% and 42±3% during periods III and IV, respectively).

When the system was supplied with eight times diluted CSS, influent $N–NH_4^+$ was removed at 75±5%
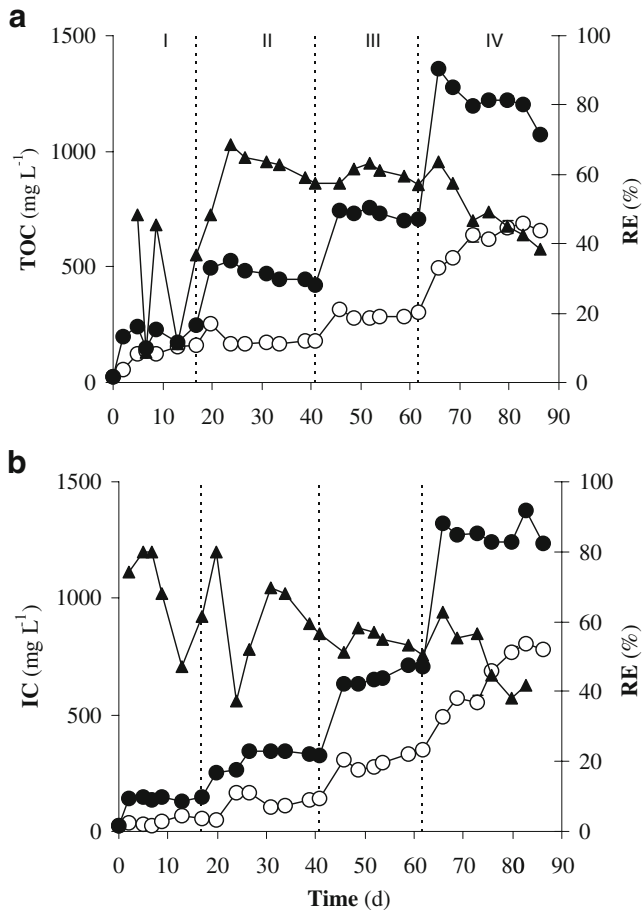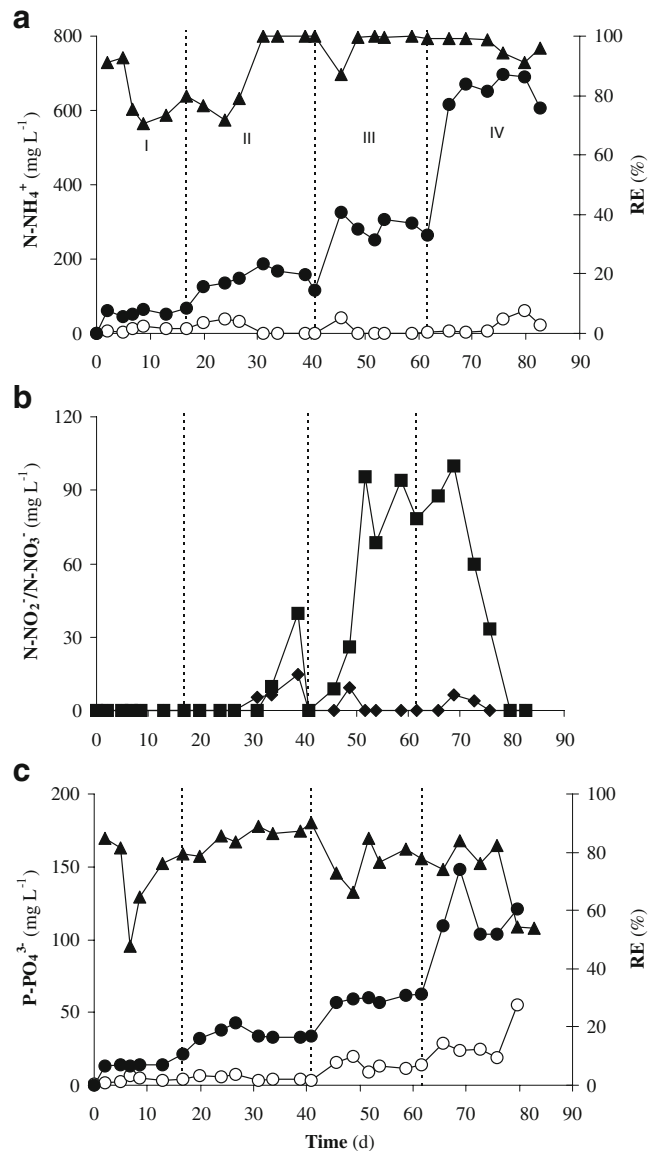
Fig. 2 Time course of TOC (**a**) and IC (**b**) concentration during the degradation of eight, four, and two times diluted and undiluted CSS (periods I, II, III, and IV, respectively). Inlet and outlet values are represented by *closed* and *open circles*, respectively, while removal efficiencies are represented by *closed triangles*

$(7\pm1$ g N m_r^{-3} day$^{-1})$, while subsequent increases up to influent N–NH$_4^+$ concentrations of 150 and 300 mg L^{-1} during periods II and III resulted in N–NH$_4^+$–REs of approx. 100% (corresponding removal rates of 21 ± 4 and 41 ± 3 g N m_r^{-3} day^{-1}, respectively; Fig. 3a). When undiluted batch B CSS was supplied to the process (period IV—days 66–86), N–NH$_4^+$–REs slightly decreased to $94\pm3\%$ (at EC of 89 ± 5 g N–NH$_4^+$ m_r^{-3} day^{-1}). Neither nitrate nor nitrite was detected during the initial stages of the biodegradation process (period I and first week of period II; Fig. 3b). However, NO$_3^-$ and NO$_2^-$ gradually increased from day 30 up to concentrations of 40 and 15 mg N L^{-1}, respectively, by the end of period II. Further increases in CSS loading resulted in stable NO$_3^-$ concentrations of 87 ± 12 mg N L^{-1} (in the absence of significant nitrite levels) during period III. Despite preceding increases in NH$_4^+$ load resulted in increasing NO$_3^-$ levels, nitrate concentration remained approx. constant at 90 mg N L^{-1} during the first week of period IV. Unexpectedly, nitrate levels rapidly decreased below the detection limit (1 mg N L^{-1}) at 80 while

maintaining reasonable undisturbed N–NH$_4^+$–RE (from 100% to 94%; Fig. 3a). On the other hand, stable PO$_4^{3-}$ removal efficiencies of approx. 80% were rapidly achieved from the first week of experimentation and maintained regardless the CSS dilution applied (Fig. 3c). A significant decrease down to 50% was however recorded by the end of period IV (corresponding to inlet PO$_4^{3-}$ concentrations of approx. 120 mg P L^{-1}).

Process start-up was characterized by an initial decrease in DO concentration down to approx. 0.3 mg O$_2$ L^{-1} at the

Fig. 3 Time course of ammonium (**a**), nitrite and nitrate (**b**), and soluble phosphate concentration (**c**) during the degradation of eight, four, and two times diluted and undiluted CSS (periods I, II, III, and IV, respectively). Inlet and outlet NH$_4^+$ concentrations are represented by *closed* and *open circles*, respectively, nitrite by *closed diamonds*, nitrate by *close squares*, inlet and outlet PO$_4^{3-}$ by *closed* and *open circles*, respectively, while both NH$_4^+$ and PO$_4^{3-}$ removal efficiencies are represented by *closed triangles*
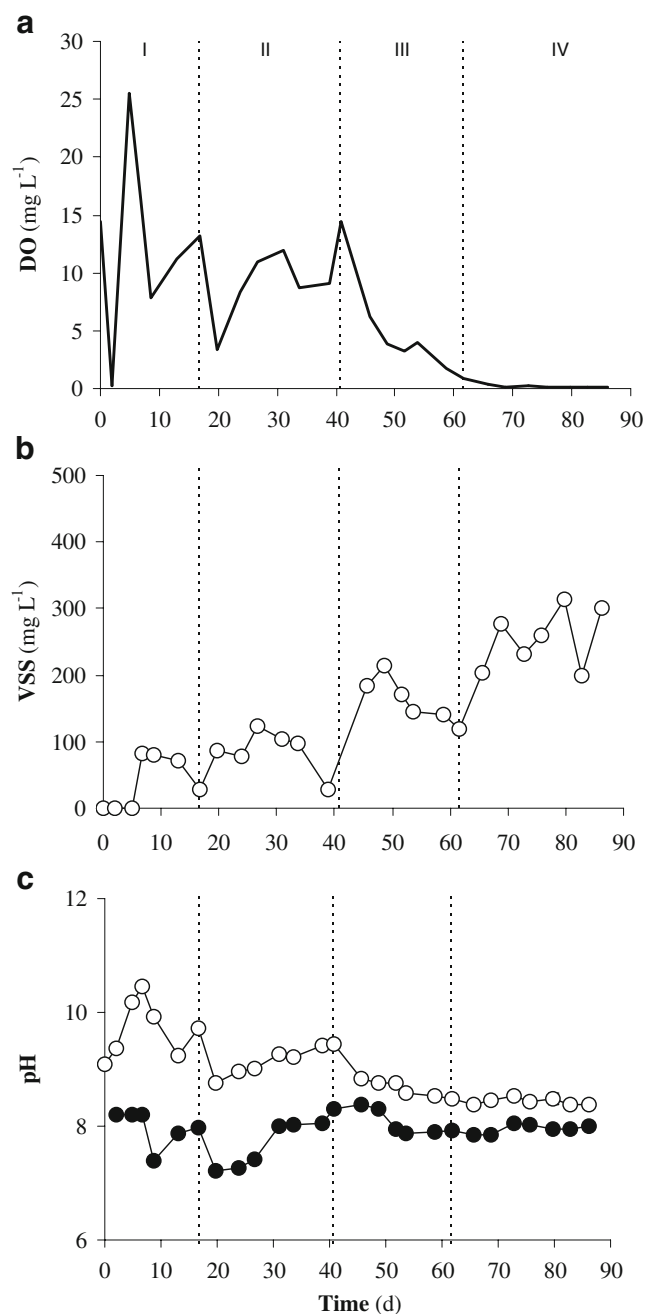
Fig. 4 Time course of dissolved oxygen concentration (**a**), volatile suspended solids (**b**), and pH (**c**) during the degradation of eight, four, and two times diluted and undiluted CSS (periods I, II, III, and IV). Inlet and outlet pH values are represented by *open* and *closed circles*, respectively

second day of experimentation, followed by a rapid rise up to 25 mg O_2 L^{-1}, to further stabilize at levels ranging from 8 to 16 mg O_2 L^{-1} (Fig. 4a). Despite that DO concentrations were never stable during the experimentation, the average concentration within each period decreased with increasing CSS loadings. Undiluted CSS feeding resulted in DO concentrations ranging from 0.1 to 0.37 mg O_2 L^{-1}.

Effluent VSS and TSS (mainly composed by *C. sorokiniana* cells; microscopical observation) were always correlated to OD_{550} measurements ($R^2 \approx 0.78$ and 0.72, respectively). Effluent VSS increased from 66 ± 25 mg L^{-1} during period I up to 268 ± 51 mg L^{-1} at period IV (Fig. 4b). The time course of photobioreactor pH was characterized by a gradually decreasing concomitant with increasing CSS loadings, from pH values of 10.5 during process start-up to pH levels of 8.4 when the process was operated with undiluted CSS (Fig. 4c).

A weak colonization of the photobioreactor's walls was observed during process start-up (period I). The increase in CSS loading from eight times diluted to four times diluted wastewater resulted in an intensive biofilm growth. In addition, a green-bluish biofilm coloration was observed from the last stages of period IV. Periodical microscopical observations of photobioreactor's effluents confirmed the predominance of *C. sorokiniana* throughout the entire experimentation and the presence of cyanobacteria by the end of period IV. In this context, swine manure centrifugation and the use of an enclosed photobioreactor severely restricted the substitution of the *C. sorokiniana* by another microalgae strain (which in addition is known as highly tolerant to high salt concentrations).

Discussion

Efficient and robust carbon, nitrogen, and phosphorous removals were achieved for over 4 months of operation in a tubular biofilm photobioreactor configuration supporting a process entirely driven by photosynthetic oxygenation (no external O_2 supply). The low surface area of the 0.5 L airtight storage tank used for recirculation resulted in an O_2 diffusion from tank headspace negligible compared to photosynthetic oxygenation. A poor process performance in terms of carbon, nitrogen, and phosphorous removal was recorded during period I, which corresponded to a phase of biomass acclimation and biofilm establishment. When the experimental system was then supplied with four and two times diluted CSS, intense biofilm growth occurred throughout the entire photobioreactor length (visual observation). Under these loading rates, the process was characterized by a complete depletion of both NH_4^+ and biodegradable soluble organic carbon concomitant with high DOs, which suggests that process performance was limited by TOC and N supply rather than photosynthetic oxygenation (Figs. 2a and 3a). Indeed, no significant differences were observed between the REs recorded in the biodegradability tests carried out with batch A CSS (yielding biodegradabilities of $54 \pm 1\%$) and the REs attained under steady photobioreactor operation. When operating with undiluted pretreated swine slurry, the

process was characterized by low DOs, which suggests that CSS biodegradation was controlled by O_2 supply and therefore microalgal activity. Despite that the TOC-REs recorded at the highest loading rate were similar to those observed in the biodegradabilities tests (39% of batch B CSS), the NH_4^+–REs slightly decreased by approx. 6% (from 100% to 94.5%). These experimental findings are in agreement with those reported by Muñoz et al. (2004, 2005). Organic carbon removal rates of up to 80 ± 5 g C m_r^{-3} day^{-1} at 7 days of HRT and inlet TOC concentrations of 1,200 mg C L^{-1} were achieved in our experimental system. These rates are comparable to those described in the literature for rapidly biodegradable soluble contaminants (116 g C m_r^{-3} day^{-1} in a suspended growth tank photo-bioreactor operated at 4.5 days of HRT and inlet salicylate concentrations of 1,000 mg L^{-1}; Muñoz et al. 2004).

Stable inorganic carbon REs of approx. 60% were achieved during most of the experimentation period, which highlighted the high photosynthetic potential of the biofilm photobioreactor configuration tested. This autotrophic metabolism of the microalgal community driving biological oxygenation constitutes a competitive advantage for the treatment of wastewaters exhibiting a low C/N ratio, such as piggery effluents. Indeed, the additional microbial growth on inorganic carbon, which averages 43% of the total carbon removed, represents an extra nutrients sink via microbial assimilation. Based on the total carbon assimilated by microalgae (IC-ECs and approx. 50% of the TOC-ECs), the superficial O_2 production rates in our experimental set-up can be easily estimated assuming a 37% microalgal C content (on a TSS basis) and 1.55 g O_2 g $algae^{-1}$ (Oswald 1988). The estimated values were 14 nmol O_2 cm^{-2} min^{-1} during period IV, which were far below the maximum O_2 transfer diffusion rate through heterotrophic biofilms (20 nmol O_2 cm^{-2} min^{-1}; Roeselers et al. 2008).

Efficient and sustained nitrogen removals ranging from 94% to 100% were achieved following a proper biofilm establishment (from week 3 onward). Algal–bacterial systems have been traditionally used in tertiary treatment

processes, exhibiting always high nutrients removal efficiencies. Thus, Fallowfield and Garret (1985) and Olguin et al. (2003) recorded NH_4^+–REs ranging from 54% to 98% in high-rate algal ponds (HRAP) treating either raw or digested swine slurry. Maximum NH_4^+–ECs of up to 89 ± 5 g N–NH_4^+ m_r^{-3} day^{-1} were attained when operating the photobioreactor with undiluted CSS. These removal rates were comparable to conventional denitrification–nitrification activated sludge configurations (105 g N–NH_4^+ m_r^{-3} day^{-1} at 10 days of HRT and inlet NH_4^+ of 1,100 mg N L^{-1}; Bortone and Piccinni 1991). In our particular case, NH_4^+ assimilation into algal–bacterial biomass represented the main nitrogen removal mechanism, accounting for 84%, 64%, and 45% of the nitrogen removed (based on an experimental nitrogen biomass content of 10%) during periods II, III, and IV, respectively, while NH_4^+ nitrification only represented 7%, 23%, and 8% at the above-referred periods. These results highlighted the potential of enclosed biofilm photobioreactors for nutrients recovery via algal–bacterial biomass production due to the intensive nutrient assimilation and the absence of NH_4^+ volatilization. A preliminary nitrogen balance showed that approx. $81\pm19\%$, $87\pm12\%$, and $90\pm6\%$ of the input nitrogen was recovered in periods I, II, III, respectively. Significantly low nitrogen recoveries ($47\pm6\%$) were however recorded during period IV. This finding, together with the lack of NO_3^- increase when increasing the influent NH_4^+ (as recorded during the preceding load raises) followed by the sharp decrease in NO_3^- concentration and the low DO levels present in the cultivation medium throughout period IV (Figs. 3b and 4a), suggested that a simultaneous nitrification–denitrification might have occurred when the photobioreactor was operated at high organic loading rates. This hypothesis was further supported by an intense bubble formation at the photo-bioreactor's wall, with the subsequent decrease in the active bioreaction volume (visual observation). In addition, GC-TCD analyses indicated that up to 94% of the above-referred gas bubbles were composed of N_2. Simultaneous nitrification–denitrification is a commonly reported phenomenon in

Fig. 5 Cross-sectional view of the tubular photobioreactor (**a**) and proposed mechanism for TOC and NH_4^+ oxidation within the biofilm attached onto the tubular photobioreactor wall (**b**). *Dashed* and *continuous lines* represent O_2 and TOC/NH_4^+ gradients inside the biofilm
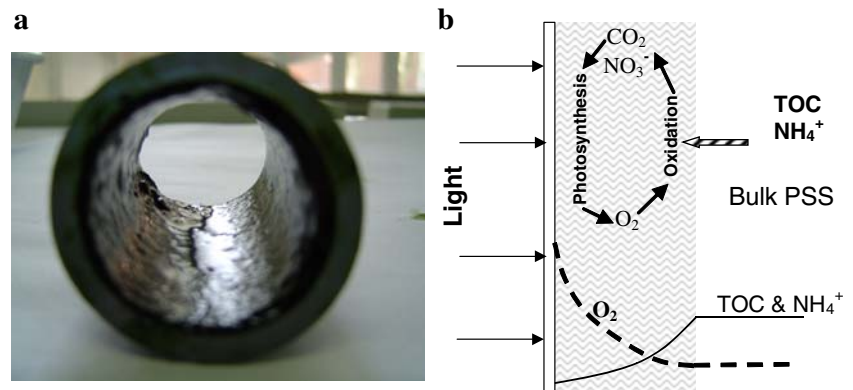
aerobic activated sludge systems due to the sharp O_2 gradients established inside biomass granules, and its occurrence within phototrophic biofilms treating high strength wastewaters must not be therefore unanticipated (Lemaire et al. 2008; De Kreuk et al. 2005).

Sustained and efficient phosphate removals (approx. 80% at inlet PO_4^{3-} concentrations of 120 mg P L^{-1}) were also recorded in the biofilm photobioreactor herein investigated. Phosphate removal performance was comparable to that described for a HRAP and conventional activated sludge processes both in terms of removal rates and removal efficiencies (Tilche et al. 1999; Olguin et al. 2003; De la Noüe and Bassères 1989). Based on a typical microalgal phosphorous content of 1.3% (Oswald 1988) and on the theoretical biomass production estimated from TOC and IC assimilation, phosphate RE of approx. 39% can be anticipated. This apparent mismatch between experimental and predicted REs might be explained by the fact that other mechanisms such as pH-induced phosphate precipitation (pH ranged from 8.5 to 9 during most of the experimentation period) were involved on phosphate removal within the photobioreactor. Indeed, the occurrence of PO_4^{3-} precipitation within algal–bacterial biofilms has been previously described by Craggs et al. (1996) in an open biofilm algal-turf scrubber treating agricultural run-off wastewaters, which increased biofilm P content up to 3% (vs a 2.1% content in our biofilm).

A cross-section of the tubular photobioreactor revealed the establishment of a thick biofilm structure at the inner wall of the tube (Fig. 5a), being the most active microalgae directly exposed to light and not directly exposed to the reactor bulk liquid. While the concentration of dissolved oxygen is expected to decrease from the photobioreactor's wall as a result of bacterial consumption through the biofilm, the concentration of TOC and NH_4^+ will however increase when approaching the bulk liquid stream. This process configuration is therefore expected to protect the active microalgae toward NH_3-mediated toxicity as a result of microalgal exposure to lower NH_4^+ concentration. This basic model of substrate transfer can be confirmed via direct O_2 microelectrode measurement, though this goal was out of the scope of this study.

Based on the elemental analysis of the algal–bacterial biofilm (C 45% and N 10% on a VSS basis), the estimated total biomass produced during periods II, III, and IV was 1,070, 1,800, and 2,870 mg VSS L^{-1} at productivities of 153, 257, and 410 mg VSS L_r^{-1} day^{-1}. These productivities were comparable to those reported in HRAPs treating diluted pretreated swine slurries (57–400 mg VSS L_r^{-1} day^{-1}; Barlow et al. 1975; Fallowfield and Garret 1985; Olguin et al. 2003). Approx. 92% of the biomass produced during the biodegradation process was retained by the combined biofilm photobioreactor + settler configuration.

Considering the low biomass concentrations recorded weekly at the bottom of the settler (no significant biomass during periods I and II and 12–18 mg SSV L^{-1} day^{-1} during periods III and IV, with 100 mL of purge withdrawn twice a week), most of the biomass accumulated in the biofilm, which might create operational problems such a tube clogging in the long-term operation. Efficient operational strategies limiting the accumulation of biomass, such as periodic increases in culture broth recirculation, must be thus implemented.

In brief, enclosed biofilm-based photobioreactors can provide with a simultaneous C, N, and P removal during the biodegradation of the pretreated swine slurry in a single-stage process. The use of centrifuged swine manure at recirculation rates of 0.14 m/s in this study allowed for a stable process operation and a quantification of the potential C, N, and P removal rates. Thus, sustained and efficient nitrogen and phosphorous removals ranging from 94% to 100% and 70–90%, respectively, were recorded in the herein-evaluated tubular biofilm photobioreactor. The particular mass transport mechanisms established in the biofilm structure (O_2 and TOC/NH_4^+ diffusing from opposite sides of the biofilm) allowed both the occurrence of simultaneous denitrification/nitrification (which, to the best of our knowledge, has not been reported before) and the protection of microalgae from any potential NH_3-mediated inhibitory effect. Despite the poor settling characteristics of *C. sorokiniana*, this biofilm-based process supported efficient biomass retention (>92% of the biomass generated during the CSS biodegradation). Further research must focus on the evaluation of this promising biotechnology long-term outdoors conditions.

References

Barlow EWR, Boersma L, Phinney HK, Miner JR (1975) Algal growth in diluted pig waste. Agr Environ 2:339–355

Baumgarten E, Nagle M, Tischner R (1999) Reduction of the nitrogen and carbon content in swine waste with algae and bacteria. Appl Microbiol Biot 52:281–284

Bortone G, Piccinni S (1991) Nitrification and denitrification in activated sludge plants for pig slurry and waste-water from cheese dairies. Bioresource Technol 37(3):243–252

Boursier H, Béline F, Paul E (2005) Piggery wastewater characterization for biological nitrogen removal process design. Bioresource Technol 96:351–358

Craggs RJ, Adey WH, Jenson KR, St John MS, Green FB, Oswald WJ (1996) Phosphorus removal from wastewater using an algal turf scrubber. Water Sci Technol 33:191–198

De Kreuk MK, Heijnen JJ, van Loosdrech M (2005) Simultaneous COD, nitrogen, and phosphate removal by aerobic granular sludge. Biotechnol Bioeng 90(6):761–769

De la Noüe J, Bassères A (1989) Biotreatment of anaerobically digested swine manure with microalgae. Biol Wastes 29:17–31

Eaton AD, Clesceri LS, Greenberg AE (2005) Standard methods for the examination of water and wastewater, 21st edn. American Public Health Association/American Water Works Association/Water Environment Federation Washington DC, USA

Evans MR, Smith MPW, Deans EA, Svoboda IF, Thacker FE (1986) Nitrogen and aerobic treatment of slurry. Agr Wastes 15:205–213

Fallowfield HJ, Garrett MK (1985) The photosynthetic treatment of pig slurry in temperate climatic conditions: a pilot-plant study. Agr Wastes 12:111–136

González C, Marciniak J, Villaverde S, García-Encina PA, Muñoz R (2008a) Microalgal-based processes for the degradation of pre-treated piggery wastewaters. Appl Microbiol Biot 80:891–898

González C, Marciniak J, Villaverde S, García-Encina PA, Muñoz R (2008b) Efficient nutrient removal from swine manure in a tubular biofilm photo-bioreactor using algae-bacteria consortia. Wat Sci Technol 58(1):95–102

Hoffman JP (1998) Wastewater treatment with suspended and nonsuspended algae. J Phycol 34:757–763

Imase M, Watanabe K, Aoyagi H, Tanaka H (2008) Construction of an artificial symbiotic community using a Chlorella-symbiotic association as a model. FEMS Microbiol Ecol 63:273–282

Lemaire R, Yuan Z, Blackall LL, Crocetti GR (2008) Microbial distribution of Accumulibacter spp. and Competibacter spp in aerobic granules from a lab-scale biological nutrient removal systems. Environ Microbiol 10(2):354–363

McGriff EC Jr, McKinney RE (1972) The removal of nutrients and organics by activated algae. Water Res 6:1155–1164

Muñoz R (2005) Algal–bacterial systems for the treatment of toxic organic pollutants" PhD Thesis. Department of Biotechnology, Lund University, Lund, Sweden.

Muñoz R, Guieysse B (2006) Algal–bacterial processes for the treatment of hazardous contaminants: a review. Water Res 40:2799–2815

Muñoz R, Köllner C, Guieysse B, Mattiasson B (2004) Photosynthetically oxygenated salicylate biodegradation in a continuous stirred tank photobioreactor. Biotechnol Bioeng 87(6):797–803

Muñoz R, Jacinto MSA, Guieysse B, Mattiasson B (2005) Combined carbon and nitrogen removal from acetonitrile using algal–bacterial reactors. Appl Microbiol Biot 67(5):699–707

Muñoz R, Díaz LF, Bordel S, Villaverde S (2007) Inhibitory effects of catechol accumulation on benzene biodegradation in Pseudomonas putida F1 cultures. Chemosphere 64:244–252

Nicolella C, Van Loosdrecht MCM, Heijnen JJ (2000) Wastewater treatment with particulate biofilm reactors. J Biotechnol 80:1–33

Nurdogan Y, Oswald WJ (1995) Enhanced nutrient removal in high rate ponds. Water Sci Technol 31:33–43

Olguin EJ, Galicia S, Mercado G, Pérez T (2003) Annual productivity of Spirulina (Arthrospira) and nutrient removal in a pig wastewater recycling process under tropical conditions. J Appl Phycol 15:249–257

Oswald WJ (1988) Micro–algae and waste-water treatment. In: Borowitzka MBL (ed) Micro-algal biotechnology. Cambridge University Press, Cambridge, pp 305–328

Roeselers G, van Loosdrecht MCM, Muyzer G (2008) Phototrophic biofilms and their potential applications. J Appl Phycol 20:227–235

Tchobanoglous G, Burton FL, Stensel HD (2003) Wastewater engineering: treatment and reuse. McGraw Hill, New York

Tilche A, Bacilieri E, Bortone G, Malaspina F, Piccinini S, Stante L (1999) Biological phosphorus and nitrogen removal in a full scale sequencing batch reactor treating piggery wastewater. Water Sci Technol 40(1):199–206

Travieso L, Benítez F, Sánchez E, Borja R, Colmenarejo MF (2006) Production of biomass (algae–bacteria) by using a mixture of settled swine and sewage as substrate. J Environ Sci Heal A 41:415–419

Wilkie AC, Mulbry WW (2002) Recovery of dairy manure nutrients by benthic freshwater algae. Bioresource Technol 84:81–91

Wolf G, Picioneraue C, van Loosdrecht M (2007) Kinetic modeling of phototrophic biofilms: the PHOBIA model. Biotechnol Bioeng 97:1064–1079